

## Electronic Supplementary Information

### Zwitterionic fused-ring framework as a new platform for heat-resistant energetic materials

Ruibing Lv,<sup>a</sup> Lan Jiang,<sup>a</sup> Jinxin Wang,<sup>a</sup> Shiliang Huang,<sup>a</sup> Siwei Song,<sup>b</sup> Liyuan Wei,<sup>a</sup> Qinghua Zhang,<sup>a,b</sup> and Kangcai Wang<sup>\*a</sup>

<sup>a</sup> Institute of Chemical Materials, China Academy of Engineering Physics (CAEP), Mianyang 621900, P. R. China.

<sup>b</sup> School of Astronautics, Northwestern Polytechnical University, Xi'an 710072, P. R. China.

Corresponding author email: wangkangcai@caep.cn (Kangcai Wang).

### Table of Contents

1. General Information .....	2
2. NMR spectra .....	3
3. IR Curves .....	4
4. X-ray Crystallography.....	5
5. Heats of formation and Physical properties .....	8
6. Thermal property analysis of ZDPT .....	9
7. Monomolecular calculation.....	10
8. Synthesis mechanism .....	12
9. References .....	12

## 1. General Information

All reagents in this study were obtained commercially and used as received. The  $^1\text{H}$  and  $^{13}\text{C}$  NMR spectra were obtained on the Bruker 400 AVANCE spectrometer (400 and 100MHz, respectively) and used internal standards ( $^1\text{H}$  NMR: 2.50ppm dimethyl sulfoxide;  $^{13}\text{C}$  NMR: 39.52ppm dimethyl sulfoxide). Infrared (IR) spectra were performed on the Perkin-Elmer Spectrum II IR Spectrometers using KBr pellets. High-resolution mass spectrometry was carried out on the Shimadzu LCMS-IT-TOF mass spectrometer using electrospray ionization (ESI). Elemental analyses (C, H, O, and N) were tested by the Vario EL III CHNOS device. Single-crystal data were collected using an Oxford Diffraction Xcalibur with a CCD detector and Cu-K $\alpha$  radiation ( $\lambda = 1.54178 \text{ \AA}$ ) using a  $\omega$  scan at room temperature. Thermal stability was carried out using a TG-DSC Mettler Toledo calorimeter equipped with an auto-cooling accessory. Using EXPLO5 (version 6.02) software to calculate the detonation parameters, including detonation velocity ( $D$ ) and detonation pressure ( $P$ ) data.<sup>1</sup> The impact and friction sensitivities were obtained by using a standard BAM Fall hammer and a BAM friction tester. The electrostatic potentials (ESPs) were obtained by using Multiwfn 3.8 software based on the calculation results via the Gaussian 16 program using B3LYP/6-31++g\*\* level,<sup>6</sup> and analyzed via Visual Molecular Dynamics (VMD, version 1.9.3) program.<sup>4</sup>

## 2. NMR spectra

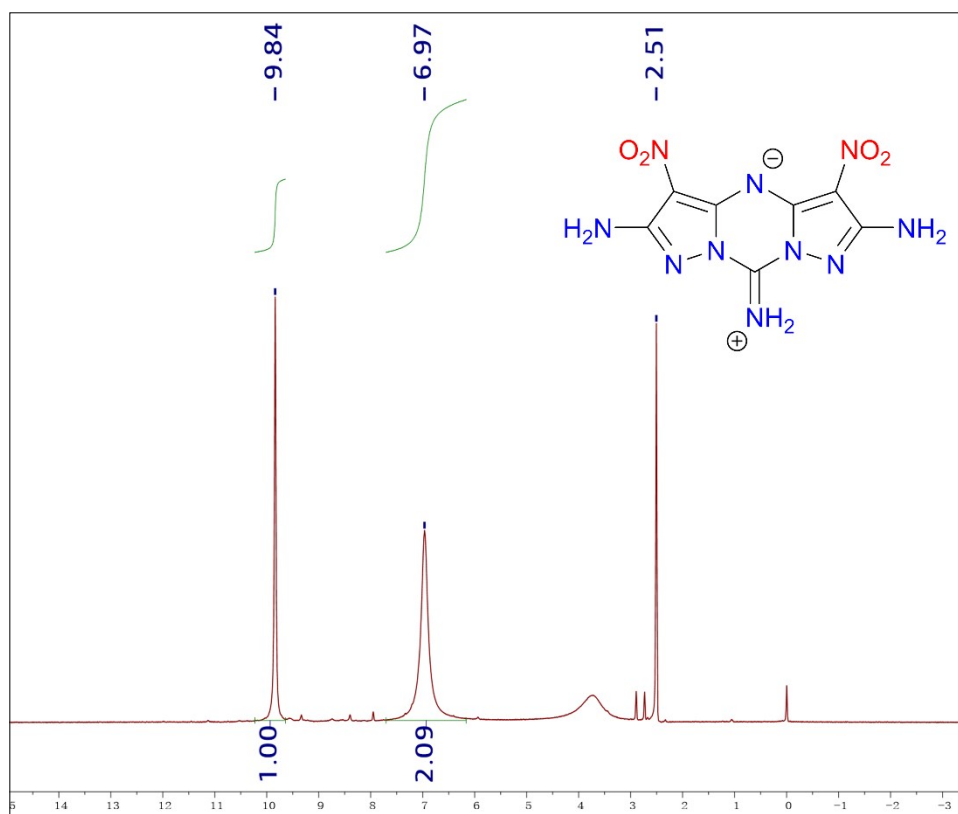


Fig. S1  $^1\text{H}$  NMR spectrum of compound ZDPT.

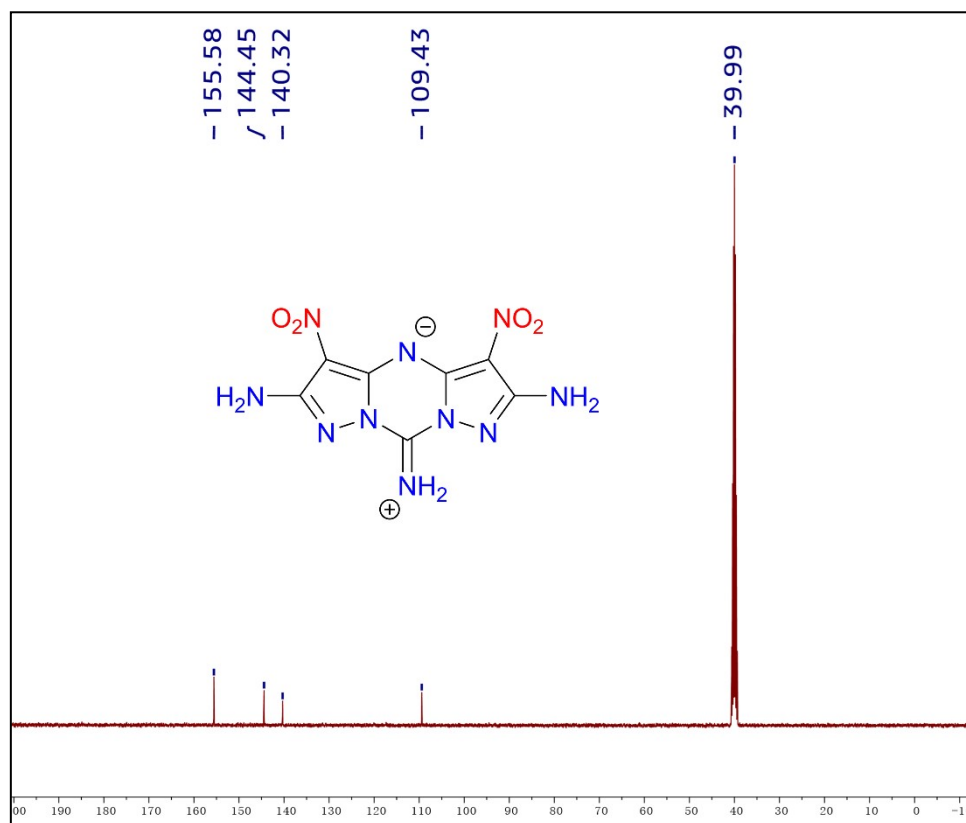


Fig. S2  $^{13}\text{C}$  NMR spectrum of compound ZDPT.

### 3. IR Curves

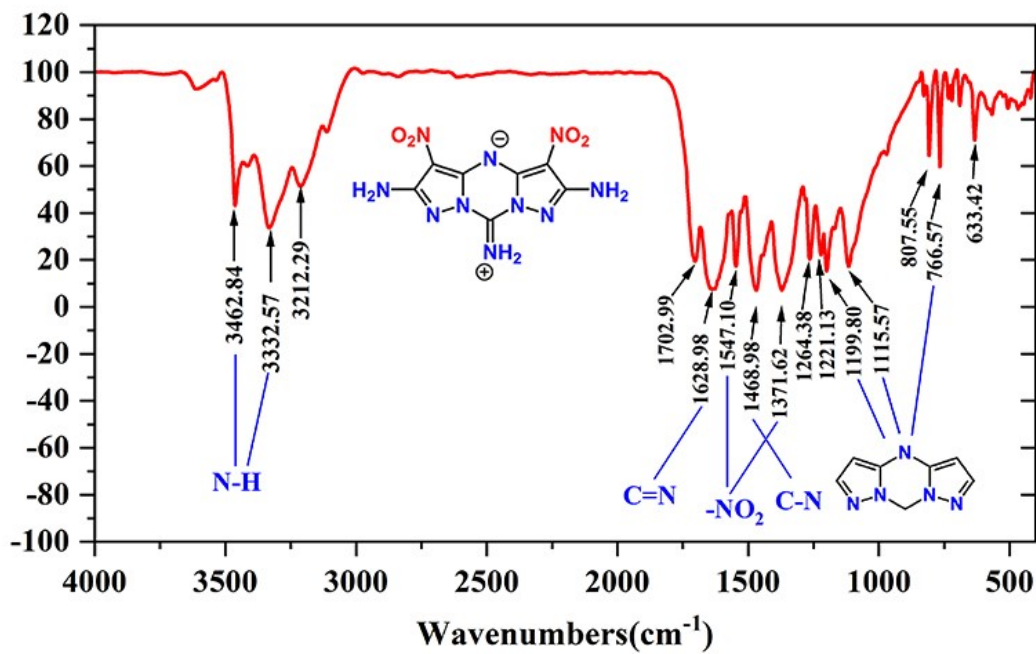
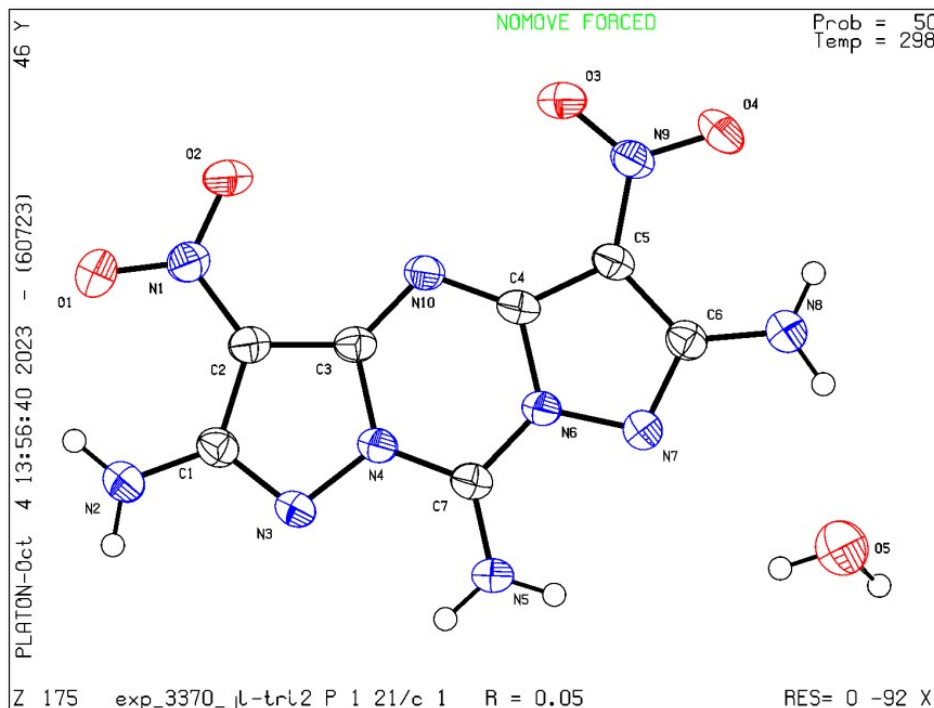


Fig. S3 IR curve of compound ZDPT.

#### 4. X-ray Crystallography

Single-crystal data were collected using an Oxford Diffraction Xcalibur with a CCD detector and Cu-K $\alpha$  radiation ( $\lambda = 1.54178 \text{ \AA}$ ) using a  $\omega$  scan at room temperature. The direct method and full-matrix least-squares method in F2 in the SHELXTL program package were used to resolve and refine the structure of these complexes. The finalized CIF file was checked with checkCIF. Illustrations of crystal structures were drawn with Diamond 3.<sup>5</sup>



**Fig.S4** The asymmetric unit of ZDPT·H<sub>2</sub>O.

**Table S1** Crystal data and details of the structure determination

<b>Compounds</b>	ZDPT·H <sub>2</sub> O
CCDC No.	2299224
Empirical formula	C <sub>7</sub> H <sub>8</sub> N <sub>10</sub> O <sub>5</sub>
Formula weight	312.23
Temperature/K	297.7(6)
Crystal system	monoclinic
Space group	<i>P</i> 2 <sub>1</sub> / <i>c</i>
<i>a</i> /Å	4.49450(10)
<i>b</i> /Å	17.2985(3)
<i>c</i> /Å	14.5787(3)
$\alpha$ /°	90
$\beta$ /°	93.648(2)
$\gamma$ /°	90
Volume/Å <sup>3</sup>	1131.17(4)
<i>Z</i>	4
$\rho$ g/cm <sup>3</sup>	1.833
$\mu$ /mm <sup>-1</sup>	1.374
<i>F</i> (000)	640.0
Crystal size/mm <sup>3</sup>	0.24 × 0.14 × 0.12
Radiation	CuK $\alpha$ ( $\lambda$ = 1.54184)
2 $\Theta$ range for data collection/°	7.94 to 155.078
Index ranges	-5 ≤ <i>h</i> ≤ 5, -21 ≤ <i>k</i> ≤ 15, -17 ≤ <i>l</i> ≤ 18
Reflections collected	8420
Independent reflections	2374 [ <i>R</i> <sub>int</sub> = 0.0700, <i>R</i> <sub>sigma</sub> = 0.0627]
Data/restraints/parameters	2374/0/207
Goodness-of-fit on <i>F</i> <sup>2</sup>	1.069
Final <i>R</i> indexes [ <i>I</i> ≥ 2 $\sigma$ ( <i>I</i> )]	<i>R</i> <sub>1</sub> = 0.0472, <i>wR</i> <sub>2</sub> = 0.1227
Final <i>R</i> indexes [all data]	<i>R</i> <sub>1</sub> = 0.0583, <i>wR</i> <sub>2</sub> = 0.1292
Largest diff. peak/hole / e Å <sup>-3</sup>	0.31/-0.22

**Table S2** Bond lengths of ZDPT·H<sub>2</sub>O.

Atom	Atom	Length/Å	Atom	Atom	Length/Å
O2	N1	1.243(2)	N1	C2	1.379(3)
O3	N9	1.231(2)	N7	C6	1.334(3)
O4	N9	1.240(2)	N3	C1	1.328(3)
N10	C4	1.338(2)	N5	C7	1.292(3)
N10	C3	1.333(2)	N9	C5	1.397(3)
N6	N7	1.383(2)	N8	C6	1.340(3)
N6	C4	1.388(2)	N2	C1	1.336(3)
N6	C7	1.352(2)	C4	C5	1.402(3)
O1	N1	1.240(2)	C3	C2	1.412(3)
N4	N3	1.389(2)	C2	C1	1.438(3)
N4	C3	1.385(2)	C5	C6	1.433(3)
N4	C7	1.344(3)			

**Table S3** Bond Angles for ZDPT·H<sub>2</sub>O.

Atom	Atom	Atom	Angle/°	Atom	Atom	Atom	Angle/°
C3	N10	C4	113.91(16)	N10	C3	N4	123.46(16)
N7	N6	C4	114.94(15)	N10	C3	C2	134.21(18)
C7	N6	N7	121.68(16)	N4	C3	C2	102.32(15)
C7	N6	C4	123.34(16)	N1	C2	C3	126.26(17)
C3	N4	N3	115.34(15)	N1	C2	C1	126.36(18)
C7	N4	N3	121.35(16)	C3	C2	C1	107.37(16)
C7	N4	C3	123.29(16)	N9	C5	C4	126.19(18)
O2	N1	C2	118.62(17)	N9	C5	C6	126.26(17)
O1	N1	O2	122.12(17)	C4	C5	C6	107.52(17)
O1	N1	C2	119.26(18)	N4	C7	N6	112.93(17)
C6	N7	N6	103.83(15)	N5	C7	N6	123.59(18)
C1	N3	N4	103.70(15)	N5	C7	N4	123.48(17)
O3	N9	O4	122.65(17)	N7	C6	N8	120.95(18)
O3	N9	C5	119.39(17)	N7	C6	C5	111.03(16)
O4	N9	C5	117.94(17)	N8	C6	C5	128.01(18)
N10	C4	N6	122.90(16)	N3	C1	N2	121.27(18)
N10	C4	C5	134.40(18)	N3	C1	C2	111.26(17)
N6	C4	C5	102.68(16)	N2	C1	C2	127.46(18)

## 5. Heats of formation and Physical properties

The enthalpy of formation of ZDPT was directly calculated using the Gaussian 09 program.<sup>3</sup> Gas phase heats of formation of ZDPT was computed on an isodesmic reaction (Fig. S6). The enthalpy of reaction was obtained by combining the M062X/6-311++G\*\* energy difference for the reactions, the scaled zero-point energies (ZPE), values of thermal correction (HT), and other thermal factors. All optimized structures were characterized to be true local energy minima without virtual frequencies on the potential energy surface.

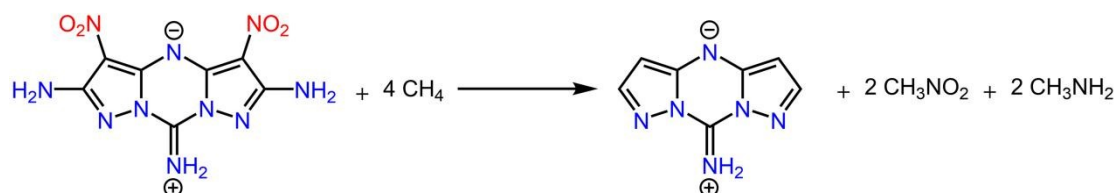


**Fig.S5** Isodesmic reactions for compound ZDPT.

The solid state heat of formation was calculated by the following equation 1. The heat of sublimation  $\Delta H_{SUB}$  was estimated by the following equation 2. T is the decomposition point temperature in Kelvin.

$$\Delta H_f(s) = \Delta H_f(g) - \Delta H_{SUB} \quad \text{(Equation 1)}$$

$$\Delta H_{SUB} = 0.188 * T \quad \text{(Equation 2)}$$

**Table S4** Physical properties of ZDPT.

Compound	ZDPT
$T_d^a$ (°C)	380
$d^b$ (g cm <sup>-3</sup> )	1.85
$\Delta_f H^c$ (kJ mol <sup>-1</sup> )	314.08
$D^d$ (m s <sup>-1</sup> )	8390
$P^e$ (GPa)	27.2
IS <sup>f</sup> (J)	>40
FS <sup>g</sup> (N)	>360

<sup>a</sup> Decomposition temperature (onset). <sup>b</sup> Experimental density. <sup>c</sup> Calculated heat of formation. <sup>d</sup> Detonation velocity. <sup>e</sup> Detonation pressure. <sup>f</sup> Impact sensitivity. <sup>g</sup> Friction sensitivity.

## 6. Thermal property analysis of ZDPT

The TG-DSC curves of ZDPT were obtained at four different heating rates of 5, 10, and 20 K min<sup>-1</sup>, respectively. Then the decomposition apparent activation energies ( $E_a$ ) of ZDPT are estimated by Ozawa (Equation 3) and Kissinger (Equation 4) methods.<sup>6</sup>

$$\log \beta = \log \left( \frac{AE_a}{Rg(a)} \right) - 2.315 - 0.4567 \frac{E_a}{RT_p} \quad (\text{Equation 3})$$

$$\ln \left( \frac{\beta}{T_p^2} \right) = \ln \frac{AR}{E_a} - \frac{E_a}{RT_p} \quad (\text{Equation 4})$$

In Equation 3 and Equation 4,  $\beta$  is the heating rate (K min<sup>-1</sup>);  $T_p$  is the decomposition peak temperature (K);  $E_a$  is the apparent activation energy (kJ mol<sup>-1</sup>);  $A$  is the pre-exponential factor;  $R$  is the ideal gas constant (J mol<sup>-1</sup> K<sup>-1</sup>). As shown in Figure 3 in article, the  $E_a$  of ZDPT obtained by the Ozawa method is 542.43 kJ mol<sup>-1</sup> and it is agreed well with the results obtained by the Kissinger method (559.56 kJ mol<sup>-1</sup>).<sup>7,8</sup> The  $R^2$  corresponding to these two methods is 0.9956 and 0.9955, respectively. (Fig.S7)

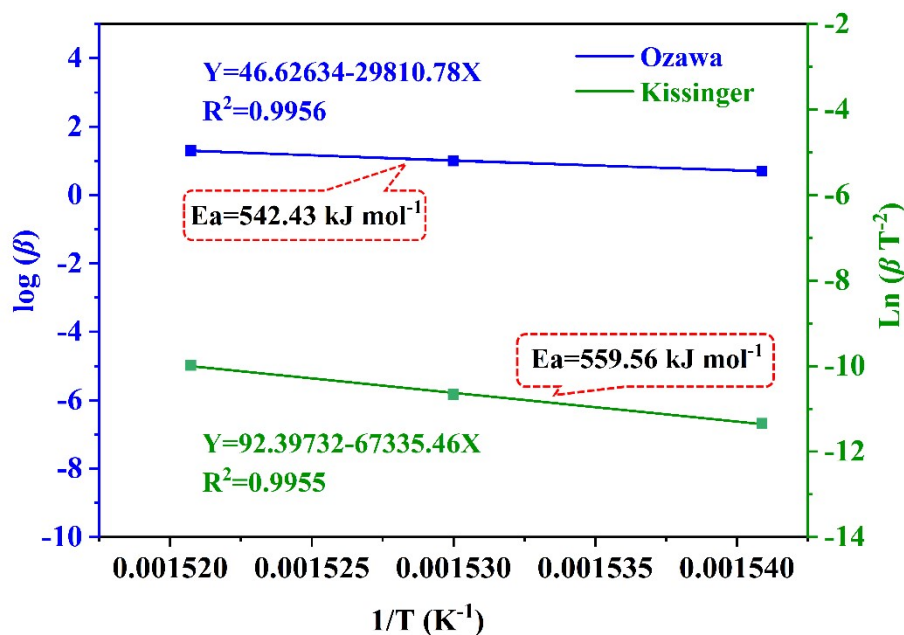


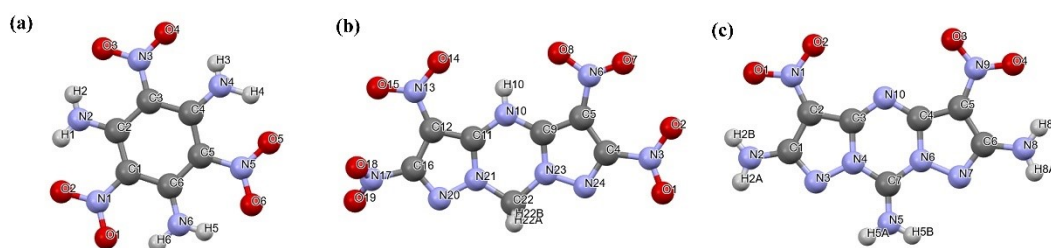
Fig.S6 The decomposition apparent activation energies of ZDPT.



## 7. Monomolecular calculation

Using the Gaussian16 and Multiwfn 3.8 program<sup>2</sup>, the geometric structures of TATB, 2,3,5,6-tetranitro-4H,9H-dipyrazolo[1,5-a:5',1'-d][1,3,5]triazine (TNDPT), and ZDPT were optimized at the B3LYP/6-31++G\*\* level. Through vibration frequency analysis, it was confirmed that these structures are the true local energy minimum on the potential energy surface without any virtual frequencies. In addition, the C-NO<sub>2</sub> bond lengths of these three compounds were shown in Table S6, corresponding to the uniform splitting bond dissociation energies (BDEs) were also calculated at the same level based on Equation 5 (Table S5 and S6).

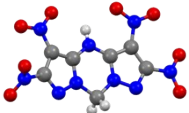
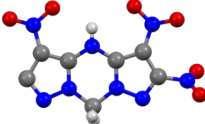


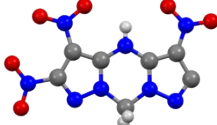
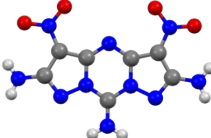
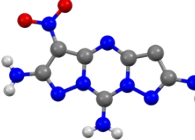


$$BDE(-NO_2) = H(NO_2) + H(\text{fragment}) - H(\text{whole}) \quad (\text{Equation 5})$$



**Fig.S7** (a) Molecular structure of TATB; (b) Molecular structure of TNDPT; (c) Molecular structure of ZDPT;

**Table S5** the energy values of each component in TATB, TNDPT, and ZDPT.

Compound	Components	Structure	Energy values/Hatree
TATB	TATB		-1011.790101
	TATB-1		-806.546684
	TATB-2		-806.546684
	TATB-3		-806.546689

	TNDPT		-1362.504073
	TNDPT-2		-1157.339252
TNDPT	TNDPT-3		-1157.324955
	TNDPT-4		-1157.324955
	TNDPT-5		-1157.339252
	ZDPT		-1118.418041
ZDPT	ZDPT-1		-913.222747
	ZDPT-2		-913.222
	-NO <sub>2</sub>		-205.071228

**Table S6** The bond lengths and BDEs of C-NO<sub>2</sub> in TATB, TNDPT, and **1** molecules

Compound	C-NO <sub>2</sub> Bond	Length/Å	BDE/Hatree	BDE/kJ·mol <sup>-1</sup>
TATB	C1-N1	1.417	0.172194	452.09
	C3-N3	1.417	0.172192	452.09
	C5-N5	1.422	0.172188	452.08
TNDPT	C4-N3	1.455	0.093599	245.74
	C5-N6	1.430	0.107896	283.28
	C12-N13	1.410	0.107893	283.27

	C16-N17	1.459	0.093593	245.72
ZDPT	C2-N1	1.379	0.124068	325.74
	C5-N9	1.397	0.124071	325.75

## 8. Synthesis mechanism

Firstly, DANP undergoes a neutralization reaction with KOH, resulting in the formation of DANP-K. Subsequently, under the influence of BrCN, DANP-K experiences a nucleophilic substitution where the pyrazole ring's negatively charged nitrogen atom attacks the BrCN molecule, leading to the departure of the -Br group and the formation of 1-Cyano-3,5-diamino-4-nitropyrazole (CNDANP). This intermediate then engages in further nucleophilic substitution and addition reactions with other DANP molecules, with the amino group of DANP attacking the C atom at the fifth position on CNDANP, and the -NH group of DANP attacking the -CN moiety of CNBANP. Following the elimination of a molecule of ammonia, this results in the cyclization to form ZDPT-K. Finally, upon acidification with HCl, the ZDPT potassium salt is converted into the ZDPT.

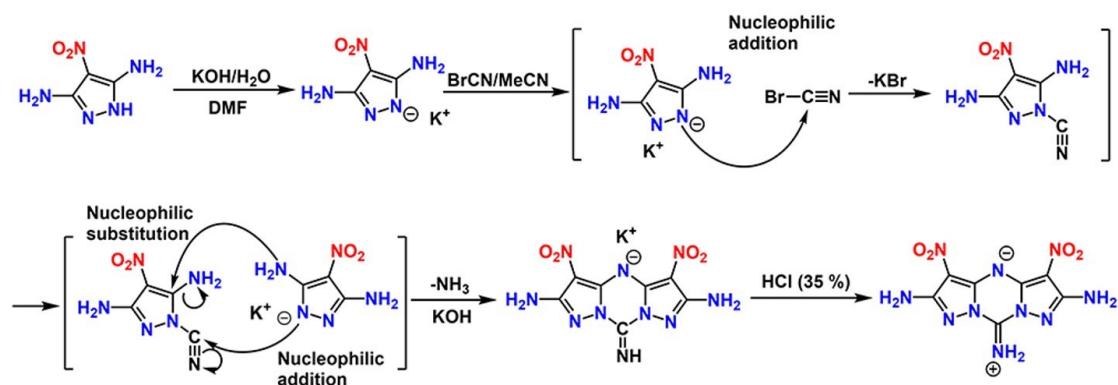


Fig. S8 Synthesis mechanism of ZDPT.

## 9. References

- 1 M. Suceca, Zagreb, Croatia, EXPLO5.
- 2 T. Lu and F. Chen, J. Comput. Chem. 2012, 33, 580-592.
- 3 Gaussian 09, Revision D. 01, M. J. Frisch et al., Gaussian Inc., Wallingford CT, 2009.
- 4 W. Humphrey, A. Dalk, K. Schulten, J. Molec. Graphics, 1996, 14, 33-38.
- 5 Diamond-Crystal and Molecular Structure Visualization Crystal Impact - Dr. H. Putz & Dr. K. Brandenburg GbR, Kreuzherrenstr. 102, 53227 Bonn, Germany.
- 6 Density Functional Theory of Atoms and Molecules, Oxford University Press, New York, 1989.
- 7 H. E. Kissinger, Anal. Chem., 1957, 29, 1702-1706.
- 8 T. Ozawa, BCSJ, 1965, 38, 1881-1886.